Changes in Mechanical Behavior During Fatigue of Semicrystalline Thermoplastics

ALAN J. LESSER*

Polymer Science and Engineering Department, University of Massachusetts, Amherst, Massachusetts 01003

SYNOPSIS

The tensile fatigue behavior of two engineering thermoplastics (polyacetal and nylon$_{6,6}$) were studied by measuring changes in the dynamic viscoelastic response together with changes in potential energy density, strain energy density, and irreversible work. The results show that both stress softening and hardening can occur in controlled load cyclic conditions. At high stress levels and/or frequencies, both the polyacetal and nylon$_{6,6}$ show evidence of thermal softening as characterized by changes in their dynamic viscoelastic properties and decrease in storage modulus with corresponding increases in loss modulus and loss tangent. This effect is supported by observed decreases in the overall crystallinity as measured in DSC experiments. At lower stress levels (the mechanically dominated region), all results indicate that, although fatigue crack propagation (FCP) is one of the mechanisms governing the fatigue life, its contribution is minor and crack initiation time constitutes the majority of the fatigue life. Also, during the initiation stage, both materials become less viscoelastic and more elastic. This phenomenon is evidenced by overall reductions in the loss modulus, loss tangent, and irreversible work densities while the storage modulus is maintained.

INTRODUCTION

Today, engineering thermoplastics are commonplace in many structurally demanding applications. They are used for pipes, for automotive components, and a wide variety of other structural and mechanical components (e.g., gears pumps). Usually these materials are chosen for either their high specific strength and toughness, their inherent resistance to corrosion in aggressive environments, or for fabrication advantages. Yet in comparison to other structural materials (e.g., metals) little is known about the mechanisms which govern their fatigue life.

The mechanisms governing the fatigue life in metals have been the topic of discussion in the engineering community for over a century.[1-9] Hence, a wealth of knowledge exists which enables engineers to confidently design metal parts for applications where the loads are expected to fluctuate or cycle over their service lives.[8] A variety of studies have been conducted in metals which clearly define the effects of grain morphology and dislocations on fatigue life.[7-9] For example, the decrease in internal damping together with the increase in modulus during cyclic loading of steels have been attributed to the gradual restriction of dislocation motions.[8]

In contrast to metal alloys, relatively little is published describing the mechanisms which control the fatigue life in polymers. Many of the earlier studies are phenomenological in nature and typically focus on the development of stress-lifetime (S–N) data for specific polymer systems and loading frequencies. However, some studies have investigated the effects of different polymer morphologies and molecular architectures.[10] These studies have shown that additives (antioxidants and nucleating agents), molecular weight, and thermal history all have a dramatic effect on the fatigue life of a polymer system.[10-12]

Effects of hysteretic heating during fatigue have also been studied in polymers.[13-15] These studies have shown that the thermal effects caused from hysteretic heating dominate the low cycle fatigue

* To whom correspondence should be addressed.

Journal of Applied Polymer Science, Vol. 58, 869–879 (1995)
 CCC 0021-8995/95/050869-11

regime (i.e., at higher stress levels and frequencies) and only become less dominant in the higher cycle fatigue range (lower stress levels and frequencies). Consequently, in the low cycle regime, the fatigue life is strongly dependent on the amplitude and frequency of loading as well as the specimen size and geometry. Constable et al.[15] recognized that the fatigue life of thermoplastics can be dominated by either of these effects. As a result, they developed a model which estimates the temperature rise in a specimen due to hysteretic heating. Also, they showed that thermal fatigue failure occurs in a sample when the temperature does not stabilize and increases above the melt temperature of the polymer. In these cases, the resulting failure is usually ductile in nature. These studies have proven to be significant milestones in describing the fatigue behavior of polymeric materials in the low cycle fatigue regime (i.e., high stress levels and or high frequencies).

Fracture mechanics concepts have been applied to many polymers to describe the mechanisms which dominate the lifetime in the high cycle fatigue regime.[10,16–20] The crack growth kinetics have been compiled in the literature[10,16–20] for a wide variety of amorphous and semicrystalline polymers. It is well established that a materials resistance to fatigue crack propagation (FCP) influences its fatigue performance. But in many applications the total fatigue life includes both the time required to initiate a crack as well as the time to grow the crack to a critical size (i.e., initiation and propagation times). However, the initiation time in many engineering thermoplastics is much greater than the propagation time and quite often dominates the total life. Unfortunately, fracture mechanics principles cannot yet predict the time required to initiate a crack in these materials.

A few studies have been conducted on polymers which describe the changes induced in the material as a result of a fatigue load.[21–26] Bouda[21] found that the effects of fatigue on glassy polymers could either manifest as stress hardening or softening depending, among other things, on the particular material being investigated. He also noticed that significant changes in the dynamic viscoelastic behavior of these materials occurred as they were exposed to fatigue. Similarly, Takahara et al. in numerous investigations[22–24] measured changes in the viscoelastic response of a variety of different polymer systems and observed changes in the storage and loss moduli during fatigue. More recently, Sakurai et al.[26] conducted a comprehensive investigation of changes induced in polyurethanes subjected to fatigue. They presented dramatic evidence of microstructural changes occurring after a fatigue load was applied. These changes were attributed to changes in crystallinity in addition to dissociation of the hard-segment microdomains. Hence, a realistic model which describes the initiation of cracks in polymers subjected to fatigue must take these effects into account.

This paper summarizes results from the first stage of an investigation whose aim is to elucidate the mechanisms of fatigue which govern the fatigue life in engineering thermoplastics. Herein, two commonly used engineering thermoplastics were selected for investigation; Celcon M90 (polyacetal copolymer supplied by Celenese) and Zytel 101 ($nylon_{6,6}$ supplied by Dupont). These thermoplastics were selected because they are used in a wide variety of applications and have comparable fatigue performances as published in earlier literature.[10] We present experimental results from *in situ* measures of irreversible deformation, the solid-state viscoelastic response, and the energetics (i.e., strain energy density, potential energy density, irreversible work density) during the fatigue process. These results together with other supportive analyses show that these materials can either stress soften and/or stress harden depending, among other things, on the amplitude and frequency of loading. Also, for the case of the $nylon_{6,6}$, we show that instabilities can occur over instances in time during the fatigue process which alter the materials resistance to further fatigue and do not necessarily lead to eminent failure.

EXPERIMENTAL PROCEDURE

The thermoplastics characterized in this study include a Zytel 101 ($nylon_{6,6}$, supplied by Dupont), and Celcon M90 (polyacetal copolymer supplied by Celenese). In both cases, 3.2-mm-thick ($\frac{1}{8}$-inch) ASTM D638 Type I tensile bars (illustrated in Fig. 1) were injection molded by the suppliers and provided to our department for evaluation. Both materials were conditioned for 8 weeks at 23°C and 50% relative humidity prior to testing.

All fatigue testing was conducted on an Instron Model 1321 servo-hydraulic machine in a load-controlled mode. The fatigue loads were applied in a sinusoidal fashion at a frequency of 2 Hz. This frequency was chosen on the basis of preliminary experiments with the goal being to minimize thermal effects from hysteretic heating. The maximum stress level was selected and maintained constant for individual experiments and adjusted throughout the study. The minimum stress level was maintained at

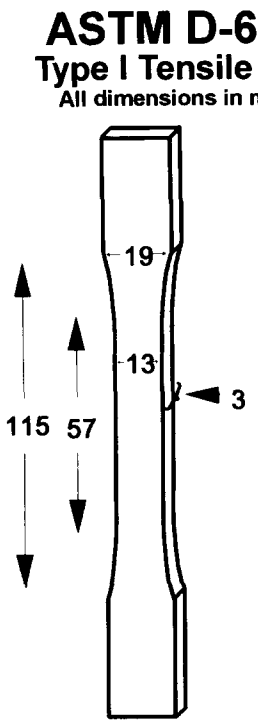

Figure 1 Schematic illustration of the *dogbone* tensile bars used in the tensile fatigue tests. The bars were injection molded to the dimensions above in accordance to the ASTM D-638 specifications.

2.2 MPa for all tests. A schematic illustration of the loading cycle is shown in Figure 2. The minimum stress level was selected to maintain a preload in the load train during the test as well as to allow for failure detection. Testing ceased when the specimens could no longer sustain a load of 1 MPa, or when the axial strain (dynamic + static) evolved beyond 100%. Also, all fatigue testing was conducted under CTCH (controlled temperature and controlled humidity; 23°C and 50%) conditions.

The Instron test frame was controlled with a Model 8500 Dynamic Test System. Using software, hysteresis loops of the crosshead load and axial strain were stored digitally for prespecified cycles (i.e., either logarithmically or periodically) through the duration of the test. Afterward, the hysteretic data were processed to calculate irreversible strain, dynamic viscoelastic parameters (E', E'', and tan δ), and energy densities for each stored cycle. The definition of these parameters is illustrated in Figure 3. The dynamic viscoelastic parameters were calculated by minimizing the error between a curve calculated using the linear viscoelastic parameters and the measured data. The energy densities (e.g., potential energy, strain energy, and irreversible work densities) were calculated through direct integration of specific parts of the hysteresis loops as shown in Figure 3.

Differential scanning calorimetry (DSC) studies were conducted on the materials prior to testing and after exposure to the fatigue test. All analyses were conducted on a DuPont Model 910 differential scanning calorimeter with a Model 9900 computer/thermal analyzer. Samples were prepared for DSC by freeze fracturing the gage area of the ASTM D638 tensile bar in liquid nitrogen and selecting 5–10 mg samples for analysis. The analyses were started at an initial temperature of −20°C and heated at a rate of 20°C/min. The polyacetal samples were taken to a maximum temperature of 210°C and the nylon$_{6,6}$ samples were taken to a maximum temperature of 310°C.

RESULTS AND DISCUSSION

S–N Curves

Figure 4 contains plots of the S–N data for the polyacetal and nylon$_{6,6}$. The ordinate and abscissa are the maximum stress (see Fig. 2) and the number of cycles to failure, respectively. Notice that both the polyacetal and nylon$_{6,6}$ display a thermally dominated region which resides at higher stress levels, and a mechanically dominated region which resides at lower levels. These regions have been reported in these materials previously[10] and are common in many polymer systems.

In the thermally dominated region the polyacetal demonstrates somewhat better fatigue resistance as compared to the nylon$_{6,6}$. Also, the transition stress level where the regions switch from thermally dominated to mechanically dominated is higher for polyacetal when compared to the nylon$_{6,6}$ (i.e., approximately 50 MPa for the polyacetal and 40 MPa for the nylon$_{6,6}$). However, caution should be ex-

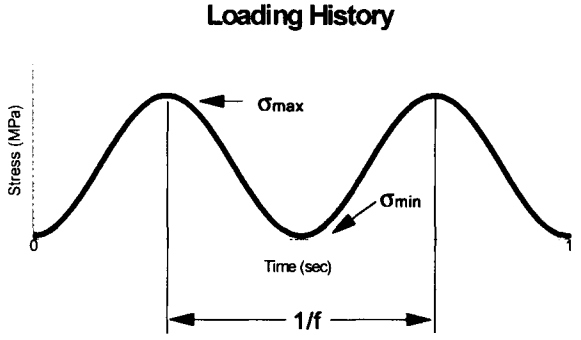

Figure 2 Illustration of the loading curves used in the controlled stress tensile fatigue tests.

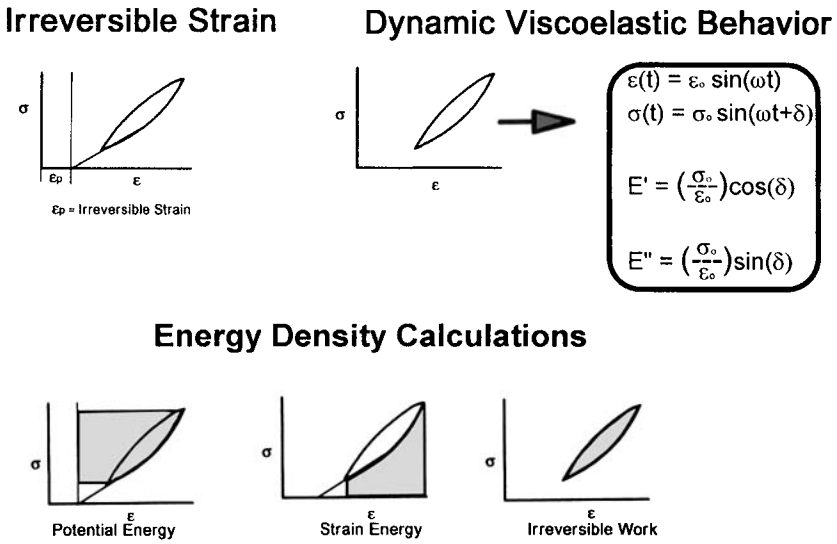

Figure 3 Schematic drawings providing definition of terms for information extracted from the fatigue hysteresis loops.

ercised when making performance-based judgments on these results since the thermally dominated region is dramatically affected by the test frequency, the test temperature, and the size and shape of the specimen.

In the mechanically dominated regions, the nylon$_{6,6}$ demonstrates somewhat better fatigue resistance when compared to polyacetal. For example, at a stress level of 30 MPa the nylon$_{6,6}$ can sustain more than 2×10^7 cycles before failure and polyacetal will last approximately 5×10^6 cycles (see Fig. 4).

If the mechanically dominated regions were governed by fatigue crack growth alone, one would expect the polyacetal to have better performance since it is more crystalline and demonstrates better resistance to subcritical fatigue crack growth.[10] On page 131, Hertzberg and Manson[10] illustrate the relative performance of various polymeric materials with regard to their fatigue crack growth kinetics. The materials presented by Hertzberg and Manson include both nylon$_{6,6}$ and polyacetal. The data are presented whereby the parameters which describe the crack growth rates for these materials can be obtained. The crack growth rates are expressed in terms of a Paris type law given by

$$\frac{da}{dN} = A(\Delta K)^m \tag{1}$$

where a is the crack length, ΔK is the change in stress intensity, N is the number of cycles, and A and m are power law coefficients. From these plots, the threshold stress intensity (K_{th}), the fracture toughness (K_{1c}), and the Paris coefficients (A and m) were extracted for both the polyacetal and nylon$_{6,6}$.

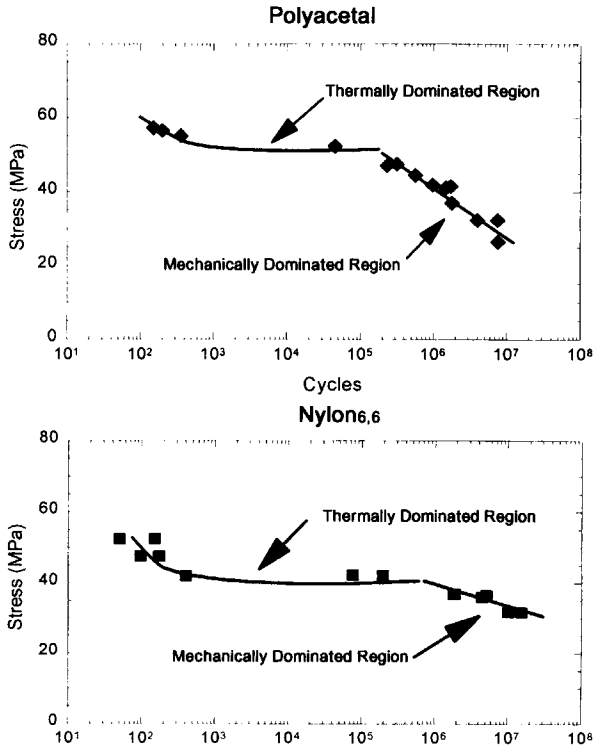

Figure 4 Plots of the fatigue stress-lifetime (S–N) curves for polyacetal (top) and nylon$_{66}$ (bottom). The stress level on the ordinate of these plots correspond to σ_{max} in Figure 2.

For the sake of comparison, consider the case when a defect initiates a crack on the surface of the specimen. The resulting equation for the stress intensity K_1 in this case can be represented by eq. (2):

$$K_1 = \sigma\sqrt{\pi a}F(a/b) \tag{2}$$

where σ is the remotely applied stress, a is the crack length, b is the specimen width, and $F(a/b)$ is a function which accounts for the specimen geometry. The function $F(a/b)$ for this geometry is available[27] and can be determined by

$$F(a/b) = \sqrt{\frac{2b}{\pi a}\tan\left(\frac{\pi a}{2b}\right)}\,\frac{0.752 + 2.02(a/b) + 0.37[1 - \sin(\pi a/2b)]^3}{\cos(\pi a/2b)} \tag{3}$$

Integration of eq. (1) to obtain an expression for the fatigue life yields the following result:

$$N_p = \int_{a_0}^{a_{cr}} \frac{da}{A(\Delta K)^m} \tag{4}$$

In eq. (4), a_0 is defined as the initial crack length (i.e., the crack length at K_{th}) and a_{cr} is the final crack length (the crack length at K_{1c}). Using eqs. (2)–(4) together with the specimen geometry and a maximum applied cyclic stress of 30 MPa, the lifetimes with regard to crack propagation were computed and compared to the fatigue data in Table I.

In Table I, K_{th} and K_{1c} are the threshold stress intensities from reference 10, A and m are the Paris law coefficients extracted from the data in reference 10, N_p is number of cycles required to propagate the crack from its threshold size to the critical length [calculated using eq. (4)], N_f is the total measured cycles to failure (from S–N curves), and N_i is the number of cycles required for crack initiation ($N_i = N_f - N_p$). Table I shows that although polyacetal has better resistance to fatigue crack growth, the nylon$_{6,6}$ has a larger overall fatigue life and consequently must have a greater resistance to crack initiation. Table I also demonstrates that the lifetimes of both of these polymer systems in the mechanically dominated regions are not due to the materials resistance to crack growth alone and that their resistance to crack initiation time plays a dominant role.

Evolution of Hysteresis Loops

In general, the hysteresis loops in polymeric materials will show stress softening effects in the thermally dominated region and will show no softening or even hardening in the mechanically dominated region. These responses are shown typically for polyacetal in Figure 5.

Notice in the thermally dominated region in Figure 5, the hysteresis loops show a progressive increase in compliance and irreversible work as the material is fatigued. This phenomenon has been reported by others[13–15] and primarily results from hysteretic heating during the fatigue process. Hysteretic heating during fatigue is inherent in many polymer systems because of the relatively high internal damping characteristics combined with the relatively low thermal conductivities present in these materials.

Figure 5 also illustrates the hysteretic behavior of polyacetal in the mechanically dominated region. Notice that, in this region, the hysteretic behavior is strikingly different. First, the material maintains its stiffness (and actually increases slightly) as it is fatigued. Also, the irreversible work (area within the hysteresis loop) decreases as the material is fatigued. Earlier studies[13–15] have attributed failure in this region to be dominated by subcritical crack growth. However, although clear evidence of fatigue crack growth can be observed on the fracture surfaces of the failed specimens, classical fracture mechanics principles alone cannot account for the observed

Table I Comparison of Fracture and Fatigue Lifetimes at a Maximum Stress of 30 MPa and a Frequency of 2 Hz

Material	K_{th} (MPa m$^{1/2}$)	K_{1c} (MPa m$^{1/2}$)	A	m	N_p	N_f	N_i
Nylon$_{6.6}$	2.0	6.0	5.4×10^{-9}	6.8	9000	2×10^7	$\sim 2 \times 10^7$
Polyacetal	2.5	3.1	1.3×10^{-17}	20.0	186000	5×10^6	$\sim 4.8 \times 10^6$

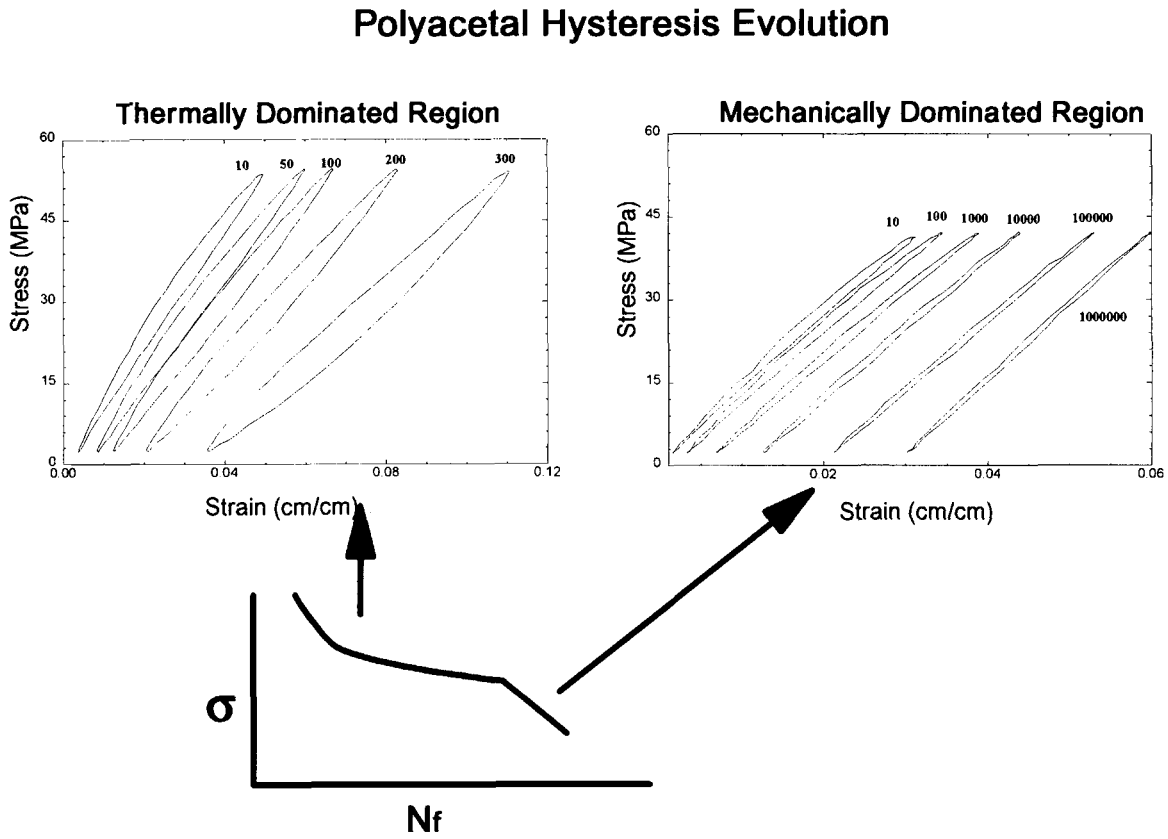

Figure 5 Plots of hysteresis loops for polyacetal fatigued in the thermally dominated region (left) and the mechanically dominated region (right). The numbers located by each hysteresis loop indicate the cycle number for that hysteresis loop.

changes in the hysteretic behavior in this region. That is, a continual increase in the compliance is expected to occur as a natural result of crack growth. Yet, over the majority of the lifetime in the mechanically dominated region, polyacetal shows no appreciable change in compliance. Hence, it is expected that other mechanisms dominate the lifetime prior to crack growth in this region.

In comparison to polyacetal, the hysteretic response of nylon$_{6,6}$ is more complex. First, no clear distinction exists between the observed phenomena in the thermally dominated and mechanically dominated regions. This observation could be due in part to the fact that a clear mechanically dominated leg in the S–N curve (Fig. 4) was not achieved within 2 $\times 10^7$ cycles. However, regardless of the region (i.e., regardless of the stress level), the hysteresis evolution show evidence of both stress softening and hardening. These phenomena occur in a sequential manner over brief segments in the lifetime, with the softening happening first followed by the hardening. An illustration of this phenomenon is shown typically for nylon$_{6,6}$ in Figure 6.

In order to investigate the changes in hysteretic behavior more closely, quantitative characterizations of the hysteretic evolutions were conducted. Each of the stored hysteresis loops were digitally processed with a computer program designed to calculate the irreversible strain, rheological properties

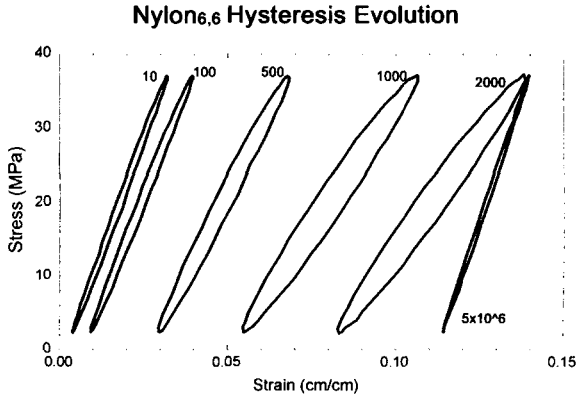

Figure 6 Plots of typical hysteresis loops for nylon$_{66}$. Notice the effects of stress softening up to cycle 2000 with subsequent stress hardening occurring beyond that.

(i.e., E', E'', and tan δ), and the energy densities (potential, strain, and irreversible work). The following sections will present the results from these analyses.

Irreversible Strain

The irreversible strain is defined herein as the permanent strain developed in the sample during fatigue. It is calculated by linearly extrapolating the lower quarter of the unloading portion of the hysteresis loop to a zero stress level (see Fig. 3).

Figure 7 presents the measured irreversible strain for six polyacetal samples fatigued at different stress levels ranging between 45 and 56 MPa. Figure 7 shows that the irreversible strains essentially increase incrementally with the applied cycles over the complete range of maximum applied stress levels. The maximum permanent strain ranged between 2 and 4% and averaged approximately 3.5%. Note that this strain is well below the failure strain measured from a uniaxial tension test (ε_f = 60%).

Figure 8 presents the irreversible strains measured in the nylon$_{6,6}$ fatigue tests. Figure 8(a) and (b) shows the same data plotted at different scales on the ordinate. The strain curves in Figure 8 correspond to maximum stress levels ranging between 35 and 44 MPa. At first glance, Figure 8(a) appears to distinguish between the deformational response in the thermal and mechanical regions. If a maximum stress is applied greater than or equal to 38 MPa (the apparent knee), the nylon$_{6,6}$ samples undergo *drawing* at prescribed instances in their lifetimes. Also, the amount of drawing is closely related to the magnitude of the applied stress. After drawing, the samples continue to sustain the fatigue load.

Below the 38 MPa knee, the nylon$_{6,6}$ first appears to fatigue continuously and undergoes no dramatic changes [Fig. 8(a)]. However, Figure 8(b) shows the same data plotted at a different strain scale. In Figure 8(b), all of the strain curves demonstrate the same behavior as those discussed previously. Consequently, the nylon$_{6,6}$ samples resist permanent strain for a period of time, then undergo brief periods of relatively large irreversible strain followed by a stable period where the material can continue to sustain the fatigue load. In some cases this process is repeated.

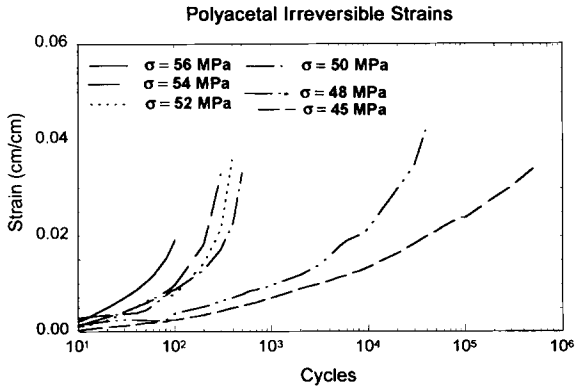

Figure 7 Plots of the irreversible strains occurring in polyacetal during fatigue at different maximum stress levels.

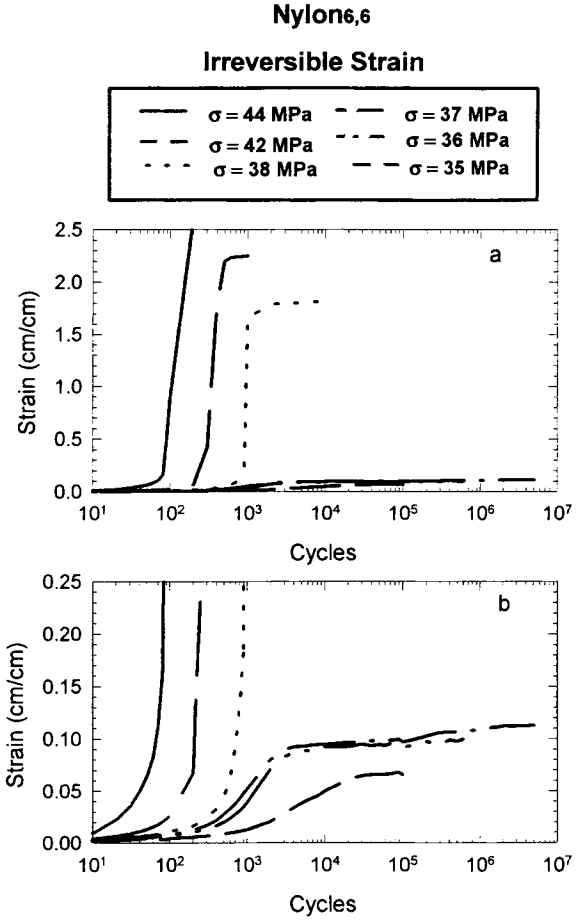

Figure 8 Plots of the irreversible strains occurring in nylon$_{66}$ during fatigue at different maximum stress levels. Graphs a and b both present the same data except that the scale on the ordinates are different. Comparison of these two graphs show that the *drawing* phenomenon occurs in both the thermally dominated and mechanically dominated regions.

Dynamic Viscoelastic Behavior

The hysteretic information was used to calculate dynamic viscoelastic parameters during the fatigue process. These parameters include the storage (E') and loss (E'') moduli, and the loss tangent (tan δ).

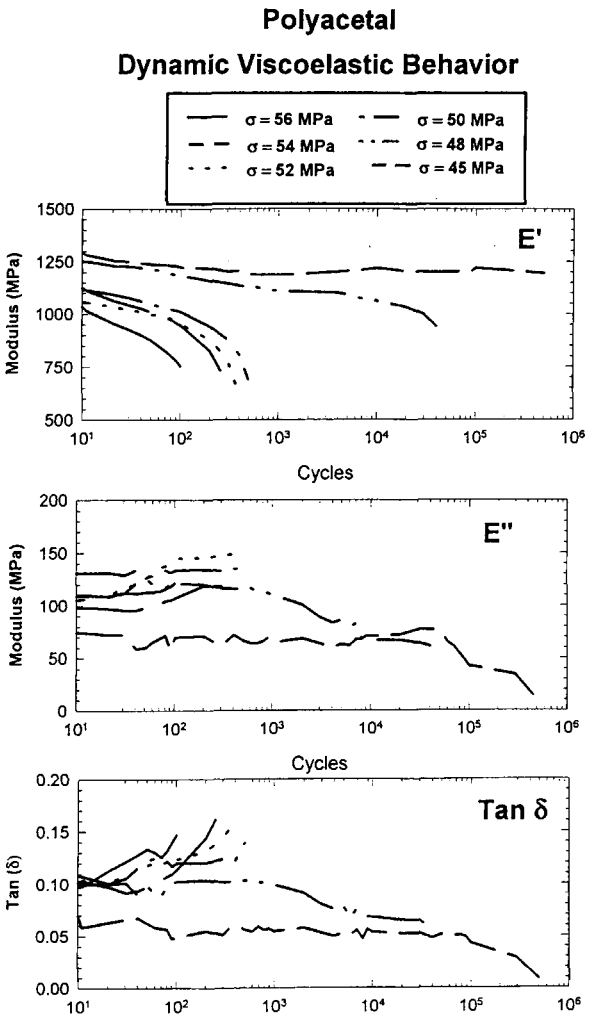

Figure 9 Graphs presenting the dynamic viscoelastic behavior for the polyacetal fatigued over a range of maximum stress levels. The top graph presents the storage moduli (E'), the middle graph presents the loss moduli (E''), and the bottom graph presents the loss tangent (tan δ).

Figure 9 presents the results for the polyacetal samples fatigued over the range of stresses discussed earlier.

Inspection of the data in Figure 9 shows that in the thermally dominated region (> 50 MPa) the storage modulus of the polyacetal decreases while the loss modulus and loss tangent increase throughout its lifetime. This is an expected response for a material whose behavior is significantly affected by hysteretic heating.

However, in the mechanically dominated region (< 48 MPa maximum stress) the material shows an initial slight drop in the storage modulus followed by a gradual increase to nearly the initial level prior to failure. The loss moduli in this same region is relatively stable at first and then decreases continually as its lifetime is exhausted. This combined effect of the moduli response results in the decline of the tan δ (Fig. 9). These curves imply that the polyacetal is becoming more elastic and less viscoelastic during the fatigue process in the mechanically dominated region.

The viscoelastic data for the nylon$_{6,6}$ are shown in Figure 10. These plots show the stress softening and subsequent hardening effects occurring at all stress levels (i.e., in both the mechanically and thermally dominated regions). Another interesting point is that the magnitude of the moduli changes in the transition regions together with the time when these transitions occur along with their duration are all strongly dependent on the maximum stress level.

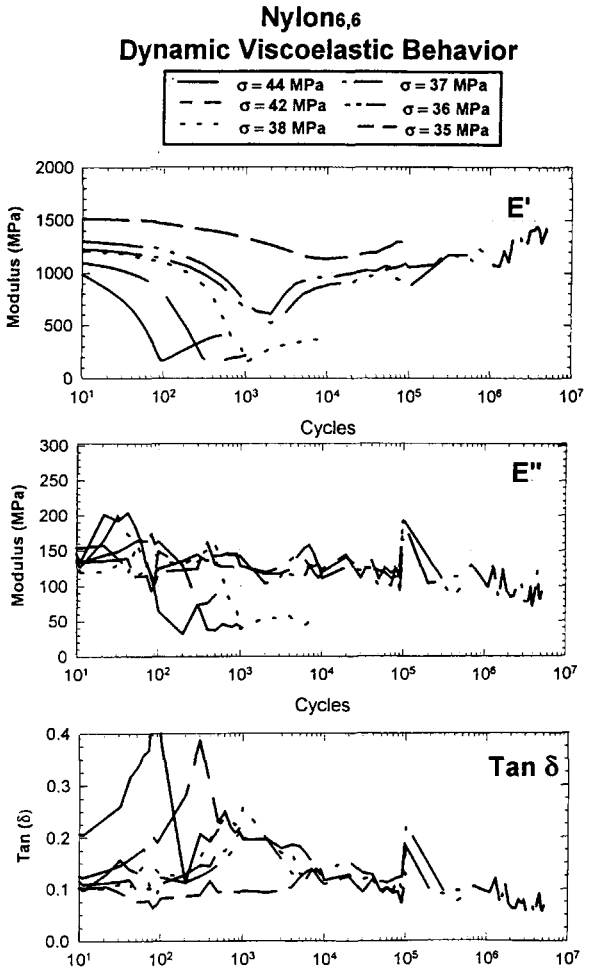

Figure 10 Graphs presenting the dynamic viscoelastic behavior for the nylon$_{66}$ fatigued over a range of maximum stress levels. The top graph presents the storage moduli (E'), the middle graph presents the loss moduli (E''), and the bottom graph presents the loss tangent (tan δ).

In contrast to the polyacetal (Fig. 9), the nylon$_{6,6}$ loss moduli and loss tangents (Fig. 10) all show a higher degree of fluctuation. The causes for these fluctuations are still under investigation, however, some general observations regarding their results can still be made. First, the loss moduli show dramatic increases followed by decreases in transition periods where the material softens and hardens. In addition there is gradual decay in the loss moduli (e.g., from 150 MPa at the start of the test to 100 MPa at failure) and loss tangents over the lifetime of the test. Consequently, the overall changes in the nylon$_{6,6}$ are similar to those measured in the polyacetal except that there are additional changes which occur over brief time segments.

Changes in Energy Densities

The potential energy density, the strain energy density, and the irreversible work densities were calculated by integrating various portions of the hysteresis loops as shown in Figure 3. Note that for the calculation of the potential energy density, the hysteresis loops are translated to a strain level such that at no applied stress no applied strain results. This adjustment is made in accordance with standard fracture mechanics methods for calculating the energy release rates for crack growth under load controlled conditions.

Figure 11 summarizes the energy density results for the polyacetal. Notice that in the thermally dominated regions all densities increase as would be expected from hysteretic heating. However, at lower stress levels (i.e., mechanically dominated region), the potential energy and strain energy densities are very uniform throughout the lifetime. This uniform performance is very attractive to material users since it implies that parts made from it will behave uniformly throughout their lifetimes. The only subtle but noticeable change in the energy densities at the lower stress levels resides in the irreversible work which shows that this material continually dissipates less energy as it approaches failure.

Another point to note is that the potential energy behavior of polyacetal at the lower stress levels (i.e., 45 MPa) shows no evidence of crack growth. That is, the energy release rates for crack growth calculated from these data would be negligible. Hence, again these results suggest that the mechanically dominated region in polyacetal is not governed by crack propagation alone.

The energy density results for the nylon$_{6,6}$ are shown in Figure 12. Notice that all the energy densities show increases, peaks, and subsequent decreases in behavior. Careful inspection of the curves shows that the energy densities (potential, strain, and irreversible work) are at a maximum at the instant that the storage and loss moduli are at their minimums. These phenomena, in turn, occur when the irreversible strain rate is at a maximum. The only conceivable way in which the energy densities could be a maximum and the corresponding moduli be a minimum is if the elastic compliance at that instant is maximized. Consequently, there is a period where the nylon$_{6,6}$ appears to behave elastomerically prior to stiffening up. Again, these effects cannot be explained with the use of conventional fracture mechanics.

Morphological Investigation

DSC analyses were conducted on selected samples of both the polyacetal and nylon$_{6,6}$ to investigate whether changes in the degree of crystallinity could be detected. The results are summarized in Table II.

The percent crystallinities calculated in the last column of Table II used latent heat of fusion data previously published.[28] The data in Table II indicate that the degree of crystallinity seems to decrease slightly as a result of exposure to fatigue at high stress levels (i.e., thermally dominated region). However, at lower stress levels (mechanically dominated regions) the materials show no evidence of reduction in crystallinity and even suggest slight increases may occur as a result. Additional studies are ongoing to identify the significance of the above measured differences.

CONCLUSIONS

Changes in the mechanical behavior have been studied during fatigue through continual monitoring and analysis of the hysteretic response polyacetal (Celcon M90) and nylon$_{6,6}$ (Zytel 101). The analysis included determinations of the irreversible strain, dynamic viscoelastic properties, and energetics of fatigue histories resulting from both thermally dominated and mechanically dominated fatigue.

The results show that both stress softening and hardening can occur in controlled load cyclic conditions. At high stress levels and/or frequencies, both the polyacetal and nylon$_{6,6}$ show evidence of thermal softening as characterized by changes in their dynamic viscoelastic properties and decrease in storage modulus with corresponding increases in loss modulus and loss tangent. This effect is further

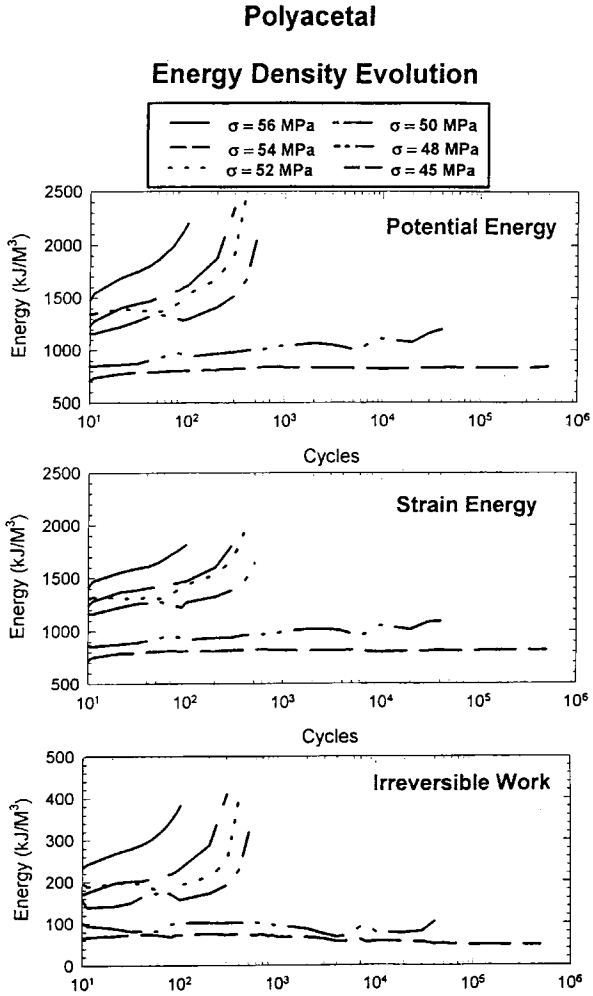

Figure 11 Graphs presenting the energy density evolution for the polyacetal fatigued over a range of maximum stress levels. The top graph presents the potential energy, the middle graph presents the strain energy, and the bottom graph presents the irreversible work densities.

supported by observed decreases in the overall crystallinity as measured in DSC experiments.

At lower stress levels (the mechanically dominated region), all results indicate that although FCP is one of the mechanisms governing the lifetime of these materials, its contribution is minor to the overall lifetime of the specimen and crack initiation time constitutes the majority of the fatigue life. Moreover, during the initiation stages both materials appear to become less viscoelastic and more elastic, this being evidenced by overall reductions in the loss modulus, loss tangent, and irreversible work densities while the storage modulus is maintained or even increases. Additional results indicate that no decreases in the degree of crystallinity can be measured in this regime (and the results may even suggest the possibility that subtle increases may occur).

Another significant point is the observation that although the polyacetal is more crystalline and has a better resistance to subcritical crack growth when compared to nylon$_{6,6}$, the nylon$_{6,6}$ has a higher overall fatigue life. This implies that in applications where cyclic or fluctuating loads are expected, the material with the greatest resistance to crack growth may not be the material which will provide for the greatest overall fatigue life. To this end, no systematic studies have yet been conducted identifying the origins of the superior fatigue performance of nylon$_{6,6}$.

Finally, the observed relatively brief instances where the nylon$_{6,6}$ undergoes stress softening followed by subsequent hardening are intriguing and still under investigation. Whether this phenomena is unique to nylon$_{6,6}$ exposed to 50% relative hu-

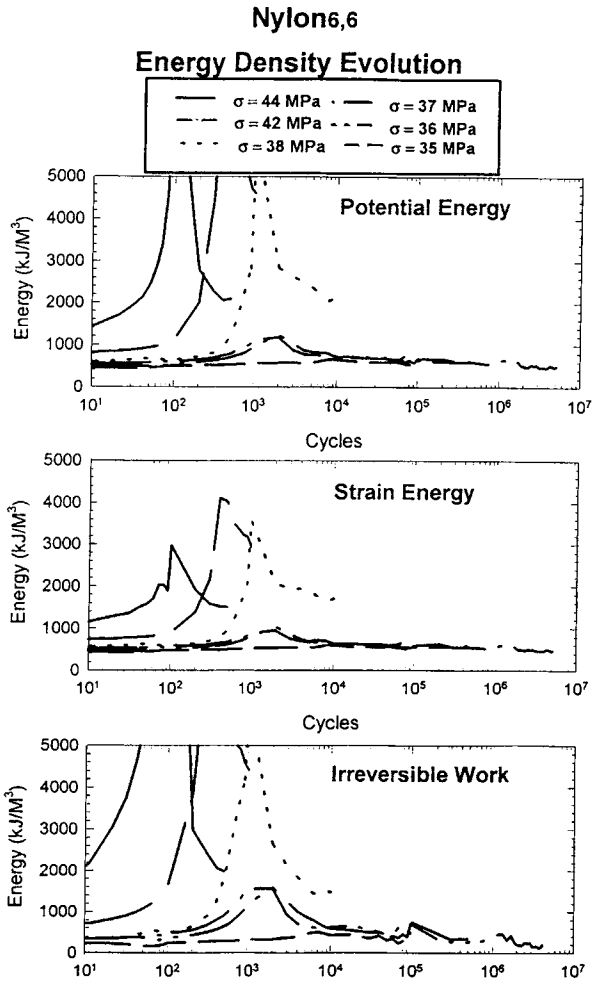

Figure 12 Graphs presenting the energy density evolution for the nylon$_{66}$ fatigued over a range of maximum stress levels. The top graph presents the potential energy, the middle graph presents the strain energy, and the bottom graph presents the irreversible work densities.

Table II Summary of DSC Scans on Polyacetal and $Nylon_{6.6}$

Material	Fatigue Stress (MPa)	Cycles to Failure	T_g (°C)	ΔH (J/g)	Crystallinity (%)
$Nylon_{6.6}$	Control	NA	58	88	43
	42	556	52	54	26
	36	5×10^6	56	99	48
Polyacetal	Control	NA	63	141	59
	56	358	64	136	57
	42	1×10^6	62	151	63

midity is not known at this time. However, it is expected that these types of transitions can create real challenges in the development of realistic models for predicting fatigue lifetimes and may severely limit the applicability of current cumulative damage theories.

REFERENCES

1. W. J. M. Rankine, *On the Causes of the Unexpected Breakage of Railway Axles; and on the Means of Preventing such Accidents by Observing the Laws of Continuity in their Construction, Proceedings Institute of Civil Engineers,* Vol. 2, London, 1843, pp. 105–108.
2. J. A. Ewing and W. Rosenhain, *Phil. Trans. Royal Soc. London Ser. A,* **193,** 353 (1900).
3. G. T. Beilby, *Proc. Royal Soc. London Ser. A,* **79,** 463 (1907).
4. J. Bauschinger, Change of Position in the Elastic Limit Under Cyclical Variations of Stress, Dingler's Journal, Bd 224: Civilingenieur, Mitthlg. des Mechanisch-Technischen Laboratoriums in Munchen, Heft, 1881, pp. XIII–XXV.
5. H. F. Moore, *Manual of Endurance of Metals under Repeated Stress,* Publication No. 18, Engineers Foundation, New York, 1927.
6. M. A. Miner, *J. Appl. Mech.,* **67,** A159 (1945).
7. P. J. E. Forsyth, in *The Mechanism of Fatigue in Aluminum and Aluminum Alloys, Fatigue in Aircraft Structures,* A. M. Freudenthal, Ed., Academic Press, New York, 1956.
8. S. S. Manson, *Avoidance, Control, and Repair of Fatigue Damage, Metal Fatigue Damage—Mechanism, Detection, Avoidance and Repair,* ASTM STP 495, American Society for Testing and Materials, 1971, pp. 254–346.
9. J. Morrow, *Cyclic Plastic Strain Energy and Fatigue of Metals,* ASTM STP 378, 1965, pp. 45–87.
10. R. W. Hertzberg and J. A. Manson, *Fatigue of Engineering Plastics,* Academic Press, New York, 1980, pp. 61–67.
11. V. G. Savkin, V. A. Belyi, T. I. Sogolova, and V. A. Kargin, *Mekh. Polim,* **2**(6), 803 (1966).
12. J. A. Sauer, E. Foden, and D. R. Morrow, *Polym. Eng. Sci.,* **17,** 246 (1977).
13. J. L. Weaver and C. L. Beatty, *Polym. Eng. Sci.,* **18**(14), 1117 (1978).
14. D. A. Opp, D. W. Skinner, and R. J. Wiktorek, *Polym. Eng. Sci.,* **9**(2), 121 (1969).
15. I. Constable, J. G. Williams, and D. J. Burns, *J. Mech. Eng. Sci.,* **12**(1), 20 (1970).
16. A. J. Kinloch and R. J. Young, *Fracture Behavior of Polymers,* Applied Science Publishers, London, 1983.
17. M. D. Skibo, R. W. Hertzberg, and J. A. Manson, *Deformation, Yield, and Fracture of Polymers, Plastics and Rubber Institute,* Cambridge, UK, 1979.
18. L. J. Broutman, *Fracture and Fatigue, Composite Materials Series,* Vol. 5, Academic Press, New York, 1974.
19. J. G. Williams, *Fracture of Polymers,* Halsted Press, New York, 1984.
20. M. G. Wyzgoski, G. E. Novak, and D. L. Simon, *J. Material Sci.,* **25,** 4501 (1990).
21. V. Bouda, *J. Polym. Sci., Polym. Phys. Ed.,* **14,** 2313 (1976).
22. A. Takahara, Y. Kenji, K. Tisato, and T. Motowo, *J. Appl. Polym. Sci.,* **25,** 597 (1980).
23. N. Kaiya, A. Takahara, and T. Kajiyama, *Polym. J.,* **22**(10), 859 (1990).
24. T. Kajiyama and A. Takahara, *Fatigue Behavior of High-Strength Polymers and Glass-Fiber Reinforced Polymer Composites Based on Dynamic Viscoelastic Measurement during the Fatigue Process,* Vol. 51(3), Memoirs of the Faculty of Engineering, Kyushu University, Japan, 1991, pp. 163–177.
25. H. Kawabe, Y. Higo, Y. Natsume, and S. Nunomura, *JSME Int. J. Ser. A,* **237**(1), 31 (1994).
26. S. Sakurai, S. Nokuwa, M. Morimoto, M. Shibayama, and S. Nomura, *Polymer,* **35**(3), 532 (1994).
27. H. Tada, P. C. Paris, and G. R. Irwin, *The Stress Analysis of Cracks Handbook,* 2nd ed., Del Research Corporation, St. Louis, MO, 1985, pp. 2.10–2.12.
28. D. W. Van Krevelen, *Properties of Polymers, Their Estimation and Correlation with Chemical Structure,* Elsevier Scientific Publishing Co., Amsterdam, 1976, pp. 574–596.

Received November 3, 1994
Accepted February 9, 1995